Japan Journal of Industrial and Applied Mathematics
https://doi.org/10.1007/s13160-024-00655-5

ORIGINAL PAPER

Heat convections in the horizontal layer with non-uniform heat supply

Hiroshi Fujiwara[1] · **Takaaki Nishida**[2]

Received: 26 September 2023 / Revised: 5 February 2024 / Accepted: 13 March 2024

Abstract
A thermal convection in horizontal fluid layer under gravity is considered. The fluid is heated from above non-uniformly. An existence theorem of stationary solutions is proved and some flow patterns are shown by numerical computations.

Keywords Thermal convection · Non-uniform heat supply · Long horizontal layer · Numerical scheme

Mathematics Subject Classification (2010) 35G60 · 76D03 · 65N06

1 Introduction

Stommel [7] considered a model of thermal convection for the fluid in the long horizontal layer $\Omega = \{ 0 < z < h\pi \ , \ 0 < x < \pi/l \}$, where the Oberbeck-Boussinesq equation is used for the fluid under the gravity. The upper surface $z = h\pi$ is maintained at the temperature $\theta_0 = t \cos(l\,x)$, $x \in (0, \pi/l)$.

In a gravity field, if uniformly heating boundary condition is posed on the top surface, no rolls appear and stability of the stationary thermal conduction solution is proved. Layer of fluid uniformly heated from below has been intensively investigated both experimentally and theoretically, and so-called Bénard convection occurs (see

Both authors contributed equally to this work

✉ Hiroshi Fujiwara
fujiwara@acs.i.kyoto-u.ac.jp

✉ Takaaki Nishida
tknish@acs.i.kyoto-u.ac.jp

[1] Department of Advanced Mathematical Sciences, Kyoto University, Yoshida-Honmachi, Sakyo-ku, Kyoto 606-8501, Kyoto, Japan

[2] Department of Advanced Mathematical Sciences, Kyoto University, Yoshida-Honmachi, Sakyo-ku, Kyoto 606-8501, Kyoto, Japan

Published online: 20 April 2024

[1, 2, 8] and references therein); more precisely, the system has bifurcation from the stationary thermal conduction solution to convective solutions where a large number of rolls are arranged uniformly.

In the present study, on the other hand, we consider non-uniform heat supply on the top surface to understand and cope with thermal convection. Stommel obtained approximate stationary solutions by asymptotic expansion of the equations with respect to a dimension-less parameter and showed its picture of contour lines of the stream function and isothermal lines. It may be considered as a simplest model of thermal effect to the ocean current.

The Stommel model can be formulated by the stream function ψ and temperature $\theta_0 + \theta$ in the following system:

$$\nu \Delta^2 \psi - \frac{\partial \psi}{\partial z}\frac{\partial \Delta\psi}{\partial x} + \frac{\partial \psi}{\partial x}\frac{\partial \Delta\psi}{\partial z} = g\alpha \frac{\partial \theta}{\partial x} + g\alpha \frac{\partial \theta_0}{\partial x} \equiv G(x,z), \quad (1)$$

$$\kappa \Delta \theta - \frac{\partial \psi}{\partial z}\frac{\partial \theta}{\partial x} + \frac{\partial \psi}{\partial x}\frac{\partial \theta}{\partial z} = -\kappa \Delta \theta_0 + \frac{\partial \psi}{\partial z}\frac{\partial \theta_0}{\partial x} \equiv F(x,z), \quad (2)$$

where ν is the dynamic viscosity, κ is the thermal diffusivity, g is the acceleration due to gravity, α is the thermal expansion in the Oberbeck approximation, and the velocities are given by

$$u = \frac{\partial \psi}{\partial z}, \qquad w = -\frac{\partial \psi}{\partial x}.$$

We here consider the case that $\theta_0(x,z)$ is independent of z and satisfies

$$\left.\frac{\partial \theta_0}{\partial x}\right|_{x=0} = \left.\frac{\partial \theta_0}{\partial x}\right|_{x=\pi/l} = 0.$$

We pose the stress free boundary conditions (3) for the stream function and Dirichlet or Neumann boundary conditions (4) for the temperature:

$$\psi|_{\partial\Omega} = 0, \quad \Delta\psi|_{\partial\Omega} = 0, \quad (3)$$

$$\begin{aligned} \theta &= 0 \ \text{ on } \{z = h\pi,\ 0 < x < \pi/l\} \\ \frac{\partial \theta}{\partial x} &= 0 \ \text{ on } \{x = 0, \pi/l,\ 0 < z < h\pi\}, \\ \frac{\partial \theta}{\partial z} &= 0 \ \text{ on } \{z = 0,\ 0 < x < \pi/l\}. \end{aligned} \quad (4)$$

Note that the boundary conditions of θ_0 and θ are implied from the adiabatic condition of the temperature $\theta_0 + \theta$ on $x = 0, \pi/l$ and $z = 0$.

Remark 1 Stommel [7] considered the fixed boundary condition on the bottom for the velocity. Instead here we use the stress free boundary condition also on the bottom, because of easy treatment for the estimates and the assumptions in the theorem which do not depend on $l \leq 1$. We hope the qualitative behavior of the solution is similar. We will treat the fixed boundary condition in a coming paper.

2 Existence of stationary solution

Proposition 1 *Let the right hand side of system* (1) *and* (2) *be given functions as* G, $F \in L^2(\Omega)$. *Then the system* (1) *and* (2) *with* (3) *and* (4) *has generalized solutions* ψ, θ *with* $\psi \in H^4(\Omega) \cap H_0^1(\Omega)$, $\theta \in H^2(\Omega)$, *such that they satisfy the following estimates in* L^2 *norm :*

$$\| \nabla \Delta \psi \| \leq \frac{\pi h}{2\nu} \| G \|, \quad \| \nabla \theta \| \leq \frac{\pi h}{\kappa} \| F \|.$$

The proof of Proposition 1 can be proceeded by the standard Galerkin method in the suitable function spaces for the existence theorem of stationary solution of Navier-Stokes equations such as Fujita [4] and Vorovich-Yudovich [9].

Theorem 2 *Let* c_0 *be the positive number in the inequality* (9). *If*

$$\frac{\pi^2 g \alpha c_0 h^3}{\nu^2} \left\| \frac{\partial \theta_0}{\partial x} \right\| \leq 1 \quad \textit{and} \quad \frac{\pi^2 g \alpha c_0 h^3}{\kappa \nu} \left\| \frac{\partial \theta_0}{\partial x} \right\| \leq \frac{1}{8},$$

then the system (1)–(4) *has a solution* $\psi \in H^4(\Omega) \cap H_0^1(\Omega)$, $\theta \in H^2(\Omega)$.

Remark 2 If the given function is $\theta_0(x, z) = t \cos(l x)$, then $\left\| \frac{\partial \theta_0}{\partial x} \right\| = \pi t \sqrt{\frac{l h}{2}}$. We notice that the length of the horizontal layer (π/l) is free from the smallness condition in the Theorem.

A proof is given by an iteration for $n = 1$ and $n + 1 = 2, 3, \cdots$ respectively.

$$\Delta^2 \psi_1 - \frac{1}{\nu} \left\{ \frac{\partial \psi_1}{\partial z} \frac{\partial \Delta \psi_1}{\partial x} - \frac{\partial \psi_1}{\partial x} \frac{\partial \Delta \psi_1}{\partial z} \right\} = \frac{g \alpha}{\nu} \frac{\partial \theta_0}{\partial x}, \tag{5}$$

$$\Delta \theta_1 - \frac{1}{\kappa} \left\{ \frac{\partial \psi_1}{\partial z} \frac{\partial \theta_1}{\partial x} - \frac{\partial \psi_1}{\partial x} \frac{\partial \theta_1}{\partial z} \right\} = -\Delta \theta_0 + \frac{1}{\kappa} \frac{\partial \psi_1}{\partial z} \frac{\partial \theta_0}{\partial x}. \tag{6}$$

$$\begin{aligned}\Delta^2 \psi_{n+1} &- \frac{1}{\nu}\left\{\frac{\partial \psi_{n+1}}{\partial z}\frac{\partial \Delta\psi_{n+1}}{\partial x} - \frac{\partial \psi_{n+1}}{\partial x}\frac{\partial \Delta\psi_{n+1}}{\partial z}\right\} \\ &= \frac{g\,\alpha}{\nu}\left\{\frac{\partial\,\theta_n}{\partial x} + \frac{\partial\,\theta_0}{\partial\,x}\right\}, \qquad (7)\\ \Delta\,\theta_{n+1} &- \frac{1}{\kappa}\left\{\frac{\partial \psi_{n+1}}{\partial z}\frac{\partial \theta_{n+1}}{\partial x} - \frac{\partial \psi_{n+1}}{\partial x}\frac{\partial \theta_{n+1}}{\partial z}\right\} \\ &= -\,\Delta\,\theta_0 + \frac{1}{\kappa}\frac{\partial \psi_{n+1}}{\partial z}\frac{\partial\,\theta_0}{\partial\,x}. \qquad (8)\end{aligned}$$

The successive approximations $\psi_{n+1}, \theta_{n+1}, \ n = 0, 1, 2, \cdots$ are obtained by Proposition 1. The convergence of this iteration is proved by the following lemmas under the assumptions of the theorem.

Lemma 3 *Let* (ψ_1, θ_1) *be the solution of* Eqs. 5 *and* 6 *with the boundary condition* (3) *and* (4). *Then we have*

$$\begin{aligned}\|\nabla\Delta\,\psi_1\| &\le \frac{\pi\,g\,\alpha\,h}{2\,\nu}\left\|\frac{\partial\,\theta_0}{\partial\,x}\right\|,\\ \|\nabla\theta_1\| &\le \left(1 + \frac{\pi\,h}{\kappa}\left\|\frac{\partial\,\psi_1}{\partial\,z}\right\|_{L^\infty}\right)\left\|\frac{\partial\,\theta_0}{\partial\,x}\right\|.\end{aligned}$$

Here we use the estimates in Proposition, integration by parts and such inequalities as

$$\|\psi\| \le \frac{\pi h}{2\sqrt{2}}\left\|\frac{\partial\psi}{\partial z}\right\|, \qquad \|\theta\| \le \frac{\pi h}{\sqrt{2}}\left\|\frac{\partial\theta}{\partial z}\right\|$$

derived from the boundary conditions (3) and (4) respectively.

Lemma 4

$$\|\nabla\psi\|_{L^\infty} \le c_0 h\,\|\Delta\nabla\psi\|, \quad \textit{where} \quad c_0^2 = \frac{1}{\pi}\sum_{n=1}^{\infty}\frac{1}{n^3}. \qquad (9)$$

Proof Suppose that $f \in L^2$ has an expansion

$$f = \sum_{m,n=1}^{\infty} f_{m,n}\sin(mlx)\sin(nz/h).$$

Noting that Parseval's theorem is given by

$$\|f\|^2 = \frac{\pi^2 h}{4l}\sum_{m,n=1}^{\infty} f_{m,n}^2,$$

it holds that

$$\|f\|_{L^\infty} \le \left\{ \sum_{m,n=1}^{\infty} f_{m,n}^2 \left\{ (ml)^2 + \left(\frac{n}{h}\right)^2 \right\}^2 \right\}^{1/2} \left\{ \sum_{m,n=1}^{\infty} \frac{1}{\left((ml)^2 + \left(\frac{n}{h}\right)^2 \right)^2} \right\}^{1/2}$$
$$= \sqrt{\frac{4lh^3}{\pi^2}}\, \|\Delta f\| \left\{ \sum_{m,n=1}^{\infty} \frac{1}{\left((mlh)^2 + n^2 \right)^2} \right\}^{1/2}.$$

The result is concluded by

$$\sum_{n=1}^{\infty}\sum_{m=1}^{\infty} \frac{1}{\left((mlh)^2 + n^2 \right)^2} \le \sum_{n=1}^{\infty} \int_0^{\infty} \frac{dx}{\left((xlh)^2 + n^2 \right)^2} = \frac{\pi}{4lh} \sum_{n=1}^{\infty} \frac{1}{n^3}.$$

□

Lemma 5 *Let* $c_0 > 0$ *be given in* Eq. 9. *If*

$$\frac{\pi\, c_0\, h^2}{\nu}\, \|\nabla\, \Delta\, \psi_n\| \le 1 \tag{10}$$

and

$$\frac{\pi^2\, g\, \alpha\, c_0\, h^3}{\kappa\, \nu} \left(\left\| \frac{\partial\, \theta_0}{\partial\, x} \right\| + \|\nabla\, \theta_n\| \right) \le \frac{1}{2}, \tag{11}$$

then we have

$$\|\nabla\, \Delta\, (\psi_{n+1} - \psi_n)\| \le \frac{1}{2}\, \|\nabla\, \Delta\, (\psi_n - \psi_{n-1})\|,$$
$$\|\nabla\, (\theta_{n+1} - \theta_n)\| \le \frac{1}{2}\, \|\nabla\, (\theta_n - \theta_{n-1})\|.$$

Proof They follow from the estimates of Proposition and the inequality (9).

$$\|\nabla\, \Delta\, (\psi_{n+1} - \psi_n)\|$$
$$\le \frac{\pi\, h}{2\, \nu} \left(\left\| \frac{\partial\, (\psi_{n+1} - \psi_n)}{\partial\, z} \frac{\partial\, \Delta \psi_n}{\partial\, x} - \frac{\partial\, (\psi_{n+1} - \psi_n)}{\partial\, x} \frac{\partial\, \Delta\, \psi_n}{\partial\, z} \right\| + g\, \alpha \left\| \frac{\partial\, (\theta_n - \theta_{n-1})}{\partial\, x} \right\| \right)$$
$$\le \frac{\pi\, c_0\, h^2}{2\, \nu}\, \|\nabla\, \Delta\, \psi_n\|\, \|\nabla\, \Delta\, (\psi_{n+1} - \psi_n)\| + \frac{\pi\, g\, \alpha\, h}{2\, \nu}\, \|\nabla\, (\theta_n - \theta_{n-1})\|,$$

$$\|\nabla\, (\theta_{n+1} - \theta_n)\|$$
$$\le \frac{\pi\, h}{\kappa} \left(\left\| \frac{\partial\, (\psi_{n+1} - \psi_n)}{\partial\, z} \frac{\partial\, \theta_n}{\partial\, x} - \frac{\partial\, (\psi_{n+1} - \psi_n)}{\partial\, x} \frac{\partial\, \theta_n}{\partial\, z} \right\| + \left\| \frac{\partial\, \theta_0}{\partial\, x} \right\| \left\| \frac{\partial\, (\psi_{n+1} - \psi_n)}{\partial\, z} \right\|_{L^\infty} \right)$$
$$\le \frac{\pi\, c_0\, h^2}{\kappa} \left(\|\nabla\, \theta_n\| + \left\| \frac{\partial\, \theta_0}{\partial\, x} \right\| \right) \|\nabla\, \Delta\, (\psi_{n+1} - \psi_n)\|.$$

Then we have by the assumption (10) on $\nabla \Delta \psi_n$

$$\| \nabla \Delta (\psi_{n+1} - \psi_n) \| \leq \frac{\pi g \alpha h}{\nu} \| \nabla (\theta_n - \theta_{n-1}) \| ,$$

Thus we have by the assumption (11)

$$\begin{aligned} \| \nabla (\theta_{n+1} - \theta_n) \| &\leq \frac{\pi c_0 h^2}{\kappa} \frac{\pi g \alpha h}{\nu} \left(\| \nabla \theta_n \| + \left\| \frac{\partial \theta_0}{\partial x} \right\| \right) \| \nabla (\theta_n - \theta_{n-1}) \| \\ &\leq \frac{1}{2} \| \nabla (\theta_n - \theta_{n-1}) \| . \end{aligned}$$

Therefore we have

$$\begin{aligned} \| \nabla \Delta (\psi_{n+1} - \psi_n) \| &\leq \frac{\pi g \alpha h}{\nu} \frac{\pi c_0 h^2}{\kappa} \left(\| \nabla \theta_n \| + \left\| \frac{\partial \theta_0}{\partial x} \right\| \right) \| \nabla \Delta (\psi_n - \psi_{n-1}) \| \\ &\leq \frac{1}{2} \| \nabla \Delta (\psi_n - \psi_{n-1}) \| . \end{aligned}$$

□

We can proceed the proof of Theorem inductively for $n = 1, 2, \cdots$. The conditions (10) and (11) hold for $n = 1$. Assume (10) and (11) hold for $n = 1, 2, \cdots, k$.

Then we have by Lemma 5

$$\begin{aligned} \| \nabla \theta_{k+1} \| &\leq \| \nabla (\theta_{k+1} - \theta_k) \| + \| \nabla (\theta_k - \theta_{k-1}) \| + \cdots + \| \nabla \theta_1 \| \\ &\leq 2 \| \nabla \theta_1 \| \leq 3 \left\| \frac{\partial \theta_0}{\partial x} \right\| , \\ \| \nabla \Delta \psi_{k+1} \| &\leq \| \nabla \Delta (\psi_{k+1} - \psi_k) \| + \| \nabla \Delta (\psi_k - \psi_{k-1}) \| + \cdots + \| \nabla \Delta \psi_1 \| \\ &\leq 2 \| \nabla \Delta \psi_1 \| \leq \frac{\pi g \alpha h}{\nu} \left\| \frac{\partial \theta_0}{\partial x} \right\| . \end{aligned}$$

Then the assumptions of Theorem give (10) and (11) for $n = k + 1$.

Therefore under strong assumptions in Theorem the successive approximation has a uniform bound in $H^3 \times H^1$ and the iteration converges to a generalized solution for our system (1)–(4).

3 Numerical scheme

This section describes an iterative scheme to find a solution to the system of non-linear (1)–(4).

We denote by k an iteration index starting from 0, and by N_x, N_z division numbers for intervals $x \in [0, \pi/\ell]$ and $z \in [0, h\pi]$, respectively. We will also use $X = \pi/\ell$, $Z = h\pi$, $\Delta x = X/N_x$ and $\Delta z = Z/N_z$. For a function f, its numerical solution $f_{i,j}$ represents the value $f(x_i, z_j)$ on a lattice point $(x_i, z_j) = (i\Delta x, j\Delta z)$.

Step 1 Set $k = 0$ and initial guess $\psi_{i,j}^0 = \theta_{i,j}^0 = 0$ for $0 \le i \le N_x, 0 \le j \le N_z$. Also set $\varphi_{i,j}^0 = u_{i,j}^0 = w_{i,j}^0 = 0$.

Step 2 Update $\varphi_{i,j}^{k+1}$, $1 \le i \le N_x - 1, 1 \le j \le N_z - 1$ by

$$\nu\left(\frac{\varphi_{i+1,j}^k - 2\varphi_{i,j}^{k+1} + \varphi_{i-1,j}^k}{\Delta x^2} + \frac{\varphi_{i,j+1}^k - 2\varphi_{i,j}^{k+1} + \varphi_{i,j-1}^k}{\Delta z^2}\right) = \frac{u_{i+1,j}^k \varphi_{i+1,j}^k - u_{i-1,j}^k \varphi_{i-1,j}^k}{2\Delta x} + \frac{w_{i,j+1}^k \varphi_{i,j+1}^k - w_{i,j-1}^k \varphi_{i,j-1}^k}{2\Delta z} + g\alpha \frac{\theta_{i+1,j}^k - \theta_{i-1,j}^k}{2\Delta x} + g\alpha \frac{\partial \theta_0}{\partial x}(x_i, z_j).$$

Step 3 Set $\varphi_{0,j}^{k+1} = \varphi_{N_x,j}^{k+1} = \varphi_{i,0}^{k+1} = \varphi_{i,N_z}^{k+1} = 0$.

Step 4 For $1 \le m \le N_x - 1, 1 \le n \le N_z - 1$, find

$$\Phi_{m,n}^{k+1} = \frac{4}{N_x N_z} \sum_{i=1}^{N_x - 1} \sum_{j=1}^{N_z - 1} \varphi_{i,j}^{k+1} \sin \frac{im\pi}{N_x} \sin \frac{jn\pi}{N_z}.$$

Then, compute $\psi_{i,j}^{k+1}$, $1 \le i \le N_x - 1, 1 \le j \le N_z - 1$, by the discrete inverse Fourier sine transform

$$\psi_{i,j}^{k+1} = -\sum_{m=1}^{N_x} \sum_{n=1}^{N_z} \frac{\Phi_{m,n}^{k+1}}{A_m^2 + B_n^2} \sin \frac{im\pi}{N_x} \sin \frac{jn\pi}{N_z},$$

where $A_m = \dfrac{m\pi}{X}$ and $B_m = \dfrac{n\pi}{Z}$.

Step 5 Calculate $u_{i,j}^{k+1}$ and $w_{i,j}^{k+1}$ by

$$u_{i,j}^{k+1} = \begin{cases} \dfrac{-3\psi_{i,0}^{k+1} + 4\psi_{i,1}^{k+1} - \psi_{i,2}^{k+1}}{2\Delta z}, & j = 0, 0 \le i \le N_x, \\ \dfrac{\psi_{i,j+1}^{k+1} - \psi_{i,j-1}^{k+1}}{2\Delta z}, & 1 \le j \le N_z - 1, 0 \le i \le N_x, \\ \dfrac{3\psi_{i,N_z}^{k+1} - 4\psi_{i,N_z-1}^{k+1} + \psi_{i,N_z-2}^{k+1}}{2\Delta z}, & j = N_z, 0 \le i \le N_x, \end{cases}$$

and

$$w_{i,j}^{k+1} = \begin{cases} -\dfrac{-3\psi_{0,j}^{k+1} + 4\psi_{1,j}^{k+1} - \psi_{2,j}^{k+1}}{2\Delta x}, & i = 0, 0 \le j \le N_z, \\ -\dfrac{\psi_{i+1,j}^{k+1} - \psi_{i-1,j}^{k+1}}{2\Delta x}, & 1 \le i \le N_x - 1, 0 \le j \le N_z, \\ -\dfrac{3\psi_{N_x,j}^{k+1} - 4\psi_{N_x-1,j}^{k+1} + \psi_{N_x-2,j}^{k+1}}{2\Delta x}, & i = N_x, 0 \le j \le N_z. \end{cases}$$

Step 6 Update $\theta_{i,j}^{k+1}$, $1 \le i \le N_x - 1$, $1 \le j \le N_z - 1$ by

$$\kappa\left(\frac{\theta_{i+1,j}^{k} - 2\theta_{i,j}^{k+1} + \theta_{i-1,j}^{k}}{\Delta x^2} + \frac{\theta_{i,j+1}^{k} - 2\theta_{i,j}^{k+1} + \theta_{i,j-1}^{k}}{\Delta z^2}\right) = \frac{u_{i+1,j}^{k+1}\theta_{i+1,j}^{k} - u_{i-1,j}^{k+1}\theta_{i-1,j}^{k}}{2\Delta x} + \frac{w_{i,j+1}^{k+1}\theta_{i,j+1}^{k} - w_{i,j-1}^{k+1}\theta_{i,j-1}^{k}}{2\Delta z} - \kappa\frac{\partial^2\theta_0}{\partial x^2}(x_i, z_j) + u_{i,j}^{k+1}\frac{\partial\theta_0}{\partial x}(x_i, z_j).$$

Step 7 Set

- $\theta_{i,N_z}^{k+1} = 0$,
- $\theta_{0,j}^{k+1} = -\frac{2}{3}\left(-2\theta_{1,j}^{k+1} + \frac{1}{2}\theta_{2,j}^{k+1}\right)$ for $1 \le j \le N_z - 1$,
- $\theta_{N_x,j}^{k+1} = \frac{2}{3}\left(2\theta_{N_x-1,j}^{k+1} - \frac{1}{2}\theta_{N_x-2,j}^{k+1}\right)$ for $1 \le j \le N_z - 1$,
- $\theta_{i,0}^{k+1} = -\frac{2}{3}\left(-2\theta_{i,1}^{k+1} + \frac{1}{2}\theta_{i,2}^{k+1}\right)$ for $0 \le i \le N_x$.

Step 8 Check a terminate criteria

$$\max_{i,j}\left\{\left|\psi_{i,j}^{k+1} - \psi_{i,j}^{k}\right|, \left|\theta_{i,j}^{k+1} - \theta_{i,j}^{k}\right|\right\} < \epsilon.$$

If so, the algorithm is finished with approximate solutions $\left\{\psi_{i,j}^{k+1}\ ;\ i, j\right\}$ and $\left\{\theta_{i,j}^{k+1}\ ;\ i, j\right\}$. Otherwise, increment k and go to Step 2.

Remark 3 Step 2 and Step 6 can be considered as Euler schemes for time evolution with $\Delta t = \frac{\Delta x^2}{4\nu}$ and $\Delta t = \frac{\Delta x^2}{4\kappa}$ respectively.

Remark 4 Step 4 corresponds to solving the boundary value problem of the Poisson equation

$$\Delta\psi^{k+1} = \varphi^{k+1}, \quad \text{in } \Omega,$$
$$\psi^{k+1} = 0, \quad \text{on } \partial\Omega$$

in the Fourier sine series as

$$\varphi^{k+1}(x_i, z_j) = \sum_{m=1}^{\infty}\sum_{n=1}^{\infty}\Phi_{m,n}^{k+1}\sin(A_m x_i)\sin(B_n z_j).$$

Therefore it has another schemes as follows.

(i) The Poisson equation can be solved by Gauss elimination.

$$\frac{\psi^{k+1}_{i+1,j} - 2\psi^{k+1}_{i,j} + \psi^{k+1}_{i-1,j}}{\Delta x^2} + \frac{\psi^{k+1}_{i,j+1} - 2\psi^{k+1}_{i,j} + \psi^{k+1}_{i,j-1}}{\Delta z^2} = \varphi^{k+1}_{i,j},$$
$$\psi^{k+1}_{0,j} = \psi^{k+1}_{N_x,j} = \psi^{k+1}_{i,0} = \psi^{k+1}_{i,N_z} = 0.$$

The results are the same as Step 4 above, but it consumes much time except for those cases with N_x and N_z being small.

(ii) The Poisson equation can be solved by similar iteration to Step 2. Update $\psi^{k+1}_{i,j}$, $1 \le i \le N_x - 1$, $1 \le j \le N_z - 1$ by

$$\frac{\psi^{k}_{i+1,j} - 2\psi^{k+1}_{i,j} + \psi^{k}_{i-1,j}}{\Delta x^2} + \frac{\psi^{k}_{i,j+1} - 2\psi^{k+1}_{i,j} + \psi^{k}_{i,j-1}}{\Delta z^2} = \varphi^{k+1}_{i,j},$$
$$\psi^{k+1}_{0,j} = \psi^{k+1}_{N_x,j} = \psi^{k+1}_{i,0} = \psi^{k+1}_{i,N_z} = 0.$$

It converges to the same solution as Step 4 only for $l = 0.001\pi$, 0.01π, and 0.05π, while it does not converge for $l = 0.5\pi$ and 0.1π.

4 Numerical examples

This section exhibits the contour lines and isothermal lines of the stationary solution obtained by numerical computations.

Throughout the section, the following constants are used:

$$h = 1/\pi, \quad g = 980, \quad \alpha = 0.0001, \quad \nu = 0.01, \quad \kappa = 0.001, \quad \text{and} \quad t = 10.$$

In computation, the following parameters are also adopted:

$$\Delta x = \Delta z = \frac{1}{256}, \quad \text{and} \quad \epsilon = 10^{-8}.$$

For the discrete sine transform (DST), `fftw_plan_r2r_2d` of FFTW3 [3] is used in Step 4. Numerical experiments are processed on Xeon Platinum 8480+ (56cores) with OpenMP parallel computation with double precision arithmetic.

Numerical experiments are performed for the following parameters:

Example 1 $l = 0.001\pi$, $N_x = 256{,}000$ $N_z = 256$.

Example 2 $l = 0.01\pi$, $N_x = 25{,}600$, $N_z = 256$.

Example 3 $l = 0.05\pi$, $N_x = 5{,}120$, $N_z = 256$.

Example 4 $l = 0.1\pi$, $N_x = 2{,}560$, $N_z = 256$.

Example 5 $l = 0.5\pi$, $N_x = 512$, $N_z = 256$.

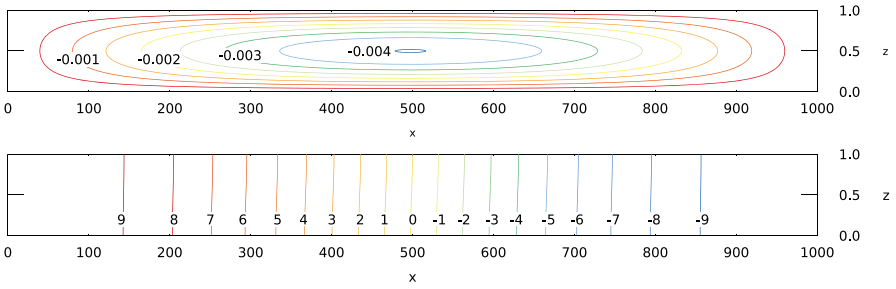

Fig. 1 Contour lines of ψ (above) and $\theta + \theta_0$ (below) with $l = 0.001\pi$ (Example 1). The former (ψ) is drawn from -0.0005 to -0.004 decreasing by 0.0005, while the latter is drawn from -9 to 9 in increments of 1

The average depth of the ocean and the distance between the equator and the pole are approximately 4 kilometers and 10,000 kilometers, respectively, and their ratio corresponds to the scale of Example 1.

Contours of numerical solutions ψ and $\theta + \theta_0$ are respectively shown in Figs. 1, 2, 3, 4, 5, and 6. Notice that $\Omega = \{0 < x < \pi/l, 0 < z < h\pi\}$ and the scale of the x-axis and z-axis is different in each figure such as $lh \ll 1$.

In Examples 1 and 2 for $lh \ll 1$, a single symmetric roll pattern appears regardless of the horizontal length of the layer. This is a significant characteristic of the present model which differs from cases of uniformly heating from the upper or bottom surfaces. From a geophysics viewpoint, it resembles the thermohaline circulation in the Atlantic ocean [6] which is formed by the warm surface ocean currents from the equator ($x = 0$) to the pole ($x = \pi/l$), cool subsurface flow in the opposite direction, and upwelling around the equator and sinking flow near the pole. It is also found that the ocean currents are moving northward along with the sea surface temperature when comparing Quick Bulletin Ocean Conditions No. 17 of 2023 and 2024 released by the Japan Coast Guard regarding ocean current and sea surface temperature near the Japanese archipelago [5]. Causes of ocean currents from the equator to the pole are complicated and include factors such as surface winds, Coriolis force, salinity, and geographical features. Our numerical results indicate that non-uniform heat supply on the top surface is also one of the contributing factors.

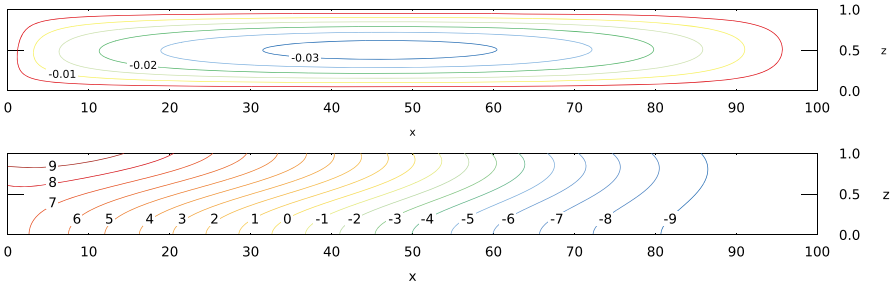

Fig. 2 Contour lines of ψ (above) and $\theta + \theta_0$ (below) with $l = 0.01\pi$ (Example 2). The former is drawn from -0.005 to -0.03 decreasing by 0.005

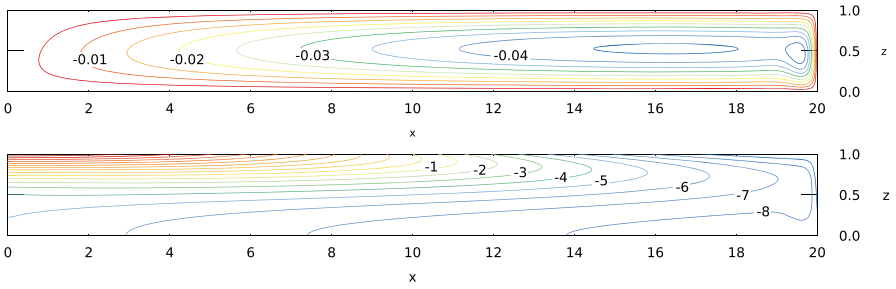

Fig. 3 Contour lines of ψ (above) and $\theta + \theta_0$ (below) with $l = 0.05\pi$ (Example 3). The profile of ψ is drawn from -0.005 to -0.035 decreasing by 0.005

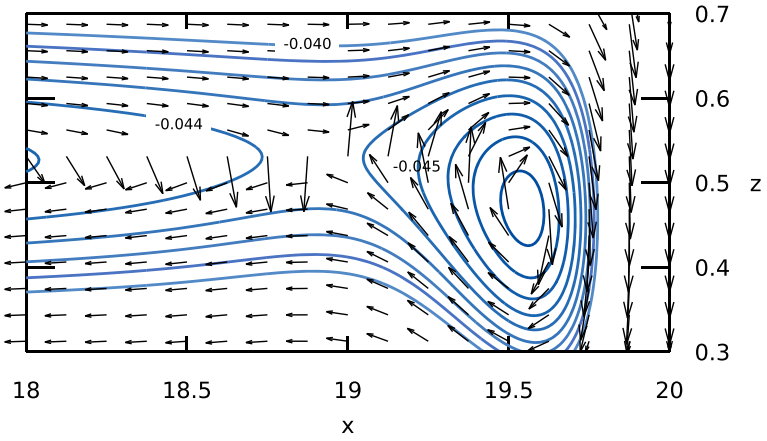

Fig. 4 Enlargement of the stream lines and velocity field of Fig. 3 for $l = 0.05\pi$. The contour are drawn from -0.040 to -0.048 decreasing by 0.001

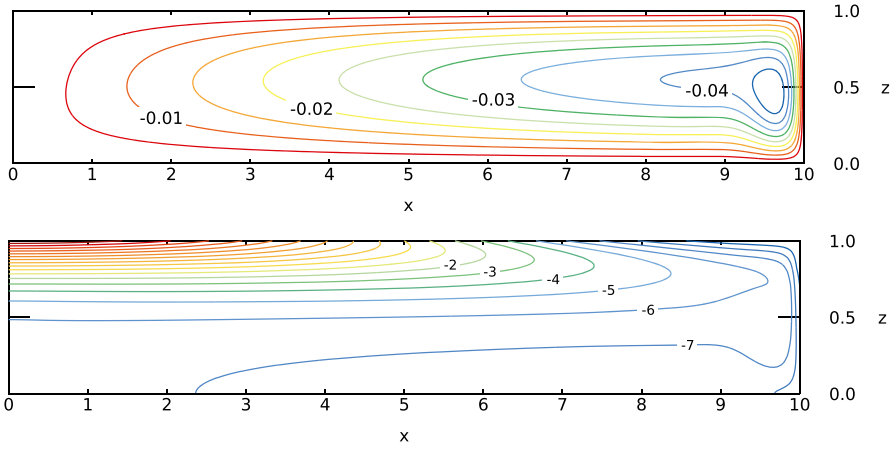

Fig. 5 Contour lines of ψ (above) and $\theta + \theta_0$ (below) with $l = 0.1\pi$ (Example 4). The profile of ψ is drawn from -0.005 to -0.045 decreasing by 0.005

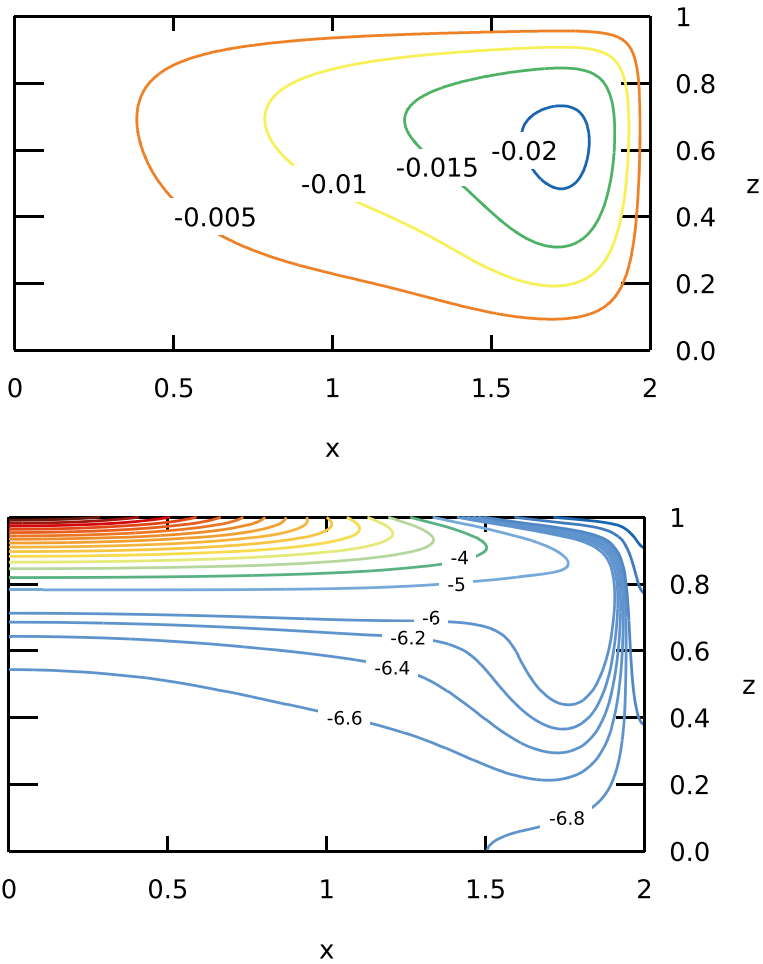

Fig. 6 Contour lines of ψ (above) and $\theta + \theta_0$ (below) with $l = 0.5\pi$ (Example 5). Contour lines of $\theta + \theta_0$ are drawn in 0.2 increments from -6 to -7, in 1 increments from 9 to -6, and -7, -8, and -9 for the rest

In numerical solution for Example 3 ($l = 0.05\pi$), a flow in the opposite direction is observed around $x = 19$, which is magnified in Fig. 4. A similar profile appears around $\pi/35 \leq l \leq \pi/16$.

When the value of l becomes larger, the roll on the right side grows and eventually occupies the entire domain. Examples 4 and 5 display an asymmetric single roll, contrasting with the case $lh \ll 1$.

It should be stressed that our numerical results imply the existence of a solution although parameters in these examples do not satisfy the condition of Theorem 2. In other words, it is strongly suggested that conditions for existence of solution in Theorem 2 can be relaxed.

Table 1 summarizes total computational time and that for DST in Examples 2–5. From the results, computational time for Example 1 is estimated to be extremely long.

Table 1 Percentage of computation time accounted for by discrete sine transform. (unit: sec.)

l/π	Computational time for DST	Total computational time	#iterations
0.01	151,775 (98%)	154,868	582,000
0.05	1,062 (67%)	1,574	473,000
0.1	494 (68%)	726	450,000
0.5	107 (66%)	162	400,000

In order to save computational time, we propose a multigrid-like strategy to generate initial guess in Step 1. Specifically, the first step is to find a numerical solution with $(N_x, N_z) = (32{,}000, 32)$. Next, the linear interpolations of the solution ψ and θ on the lattice with $(N_x, N_z) = (64{,}000, 64)$ are obtained, and corresponding u and w are computed by Step 5, and $\varphi = \Delta\psi$ by the standard five-point finite difference is computed. Using them as the initial guess, the iteration in the previous section is processed for $(N_x, N_z) = (64{,}000, 64)$. Numerical solutions for $(N_x, N_z) = (128{,}000, 128)$ and $(256{,}000, 256)$ are found recursively. The computational times are listed in Table 2, and the total computational time is 2,999 seconds, which is much less than that for $(N_x, N_z) = (64{,}000, 64)$ starting from zero initial guess.

In order to verify that numerical solutions satisfy the system of differential equations quantitatively, the residuals are examined by substituting them into the finite difference equations.

$$\max_{i,j}\left|\nu\left(\frac{\varphi^*_{i+1,j}-2\varphi^*_{i,j}+\varphi^*_{i-1,j}}{\Delta x^2}+\frac{\varphi^*_{i,j+1}-2\varphi^*_{i,j}+\varphi^*_{i,j-1}}{\Delta z^2}\right)-\left\{\frac{u^*_{i+1,j}\varphi^*_{i+1,j}-u^*_{i-1,j}\varphi^*_{i-1,j}}{2\Delta x}+\frac{w^*_{i,j+1}\varphi^*_{i,j+1}-w^*_{i,j-1}\varphi^*_{i,j-1}}{2\Delta z}+g\alpha\frac{\theta^*_{i+1,j}-\theta^*_{i-1,j}}{2\Delta x}+g\alpha\frac{\partial\theta_0}{\partial x}(x_i,z_j)\right\}\right|, \tag{12}$$

Table 2 Comparison of computational time by the initial guess for $l = 0.001\pi$. (unit: sec.)

	Zero initial guess		Interpolated initial guess	
(N_x, N_z)	Computational time	#iterations	Computational time	#iterations
(32,000, 32)	680	15,000	–	–
(64,000, 64)	12,352	48,000	869	3,220
(128,000, 128)	141,734	156,000	372	160
(256,000, 256)	–	–	1,078	50

Table 3 Residuals (12), (13), and (14) of numerical solution found by the iterative scheme in Section 3

l/π	Residual in ψ-Eq. (12)	Residual in θ-Eq. (13)	Residual in the Poisson Eq. (14)
0.001	2.22×10^{-5}	2.21×10^{-6}	4.20×10^{-7}
0.01	1.52×10^{-6}	2.61×10^{-6}	4.20×10^{-6}
0.05	5.51×10^{-6}	2.62×10^{-6}	1.51×10^{-4}
0.1	5.48×10^{-6}	2.57×10^{-6}	2.71×10^{-4}
0.5	6.52×10^{-6}	2.58×10^{-6}	3.37×10^{-4}

$$\max_{i,j}\left|\kappa\left(\frac{\theta^*_{i+1,j}-2\theta^*_{i,j}+\theta^*_{i-1,j}}{\Delta x^2}+\frac{\theta^*_{i,j+1}-2\theta^*_{i,j}+\theta^*_{i,j-1}}{\Delta z^2}\right)-\left\{\frac{u^*_{i+1,j}\theta^*_{i+1,j}-u^*_{i-1,j}\theta^*_{i-1,j}}{2\Delta x}+\frac{w^*_{i,j+1}\theta^*_{i,j+1}-w^*_{i,j-1}\theta^*_{i,j-1}}{2\Delta z}-\kappa\frac{\partial^2\theta_0}{\partial x^2}(x_i,z_j)+u^*_{i,j}\frac{\partial\theta_0}{\partial x}(x_i,z_j)\right\}\right|, \tag{13}$$

and

$$\max_{i,j}\left|\frac{\psi^*_{i+1,j}-2\psi^*_{i,j}+\psi^*_{i-1,j}}{\Delta x^2}+\frac{\psi^*_{i,j+1}-2\psi^*_{i,j}+\psi^*_{i,j-1}}{\Delta z^2}-\varphi^*_{i,j}\right|, \tag{14}$$

where lattice functions with symbol $*$ denote obtained numerical solutions. The residuals in Table 3 are sufficiently small, thus it is concluded that numerical solutions give reasonable approximations.

Remark 5 Configurations in Example 1 may be considered as a situation of a primitive equation with the assumption of static pressure because our numerical solution satisfies

$$\frac{\partial p}{\partial z}(x,z)\approx q(x),$$

for some function q which is independent of z.

Acknowledgements Nishida would like to thank Professor Tetsu Makino (Yamaguchi University), who informed me the paper of Stommel. Without the discussions and suggestions from him this work did not start. Nishida is supported in part by JSPS Kakenhi No. 20K03699 and No. 23K03165. Fujiwara is supported in part by JSPS Kakenhi No. 19H00641, No. 20H01821 and No. 22K18674.

References

1. Busse, F.H.: Non-linear properties of thermal convection. Rep. Prog. Phys. **41**, 1929–1967 (1978). https://doi.org/10.1088/0034-4885/41/12/003
2. S. Chandrasekhar, "Hydrodynamic and hydromagnetic stability", Clarendon Press, 1961
3. Frigo, M., Johnson, S.G.: The design and implementation of FFTW3. Proc. IEEE **93**(2), 216–231 (2005). https://doi.org/10.1109/JPROC.2004.840301
4. Fujita, H.: On the existence and regularity of the Steady-state solutions of the Navier-Stokes equation. J. Fac. Sci. Univ. Tokyo **1A**(9), 59–102 (1961)
5. Hydrographic and Oceangraphic Department, Japan Coast Guard. Quick bulletin of ocean conditions. https://www1.kaiho.mlit.go.jp/KANKYO/KAIYO/qboc/index_E.html. Accessed 6 Feb 2024
6. Jet Propulsion Laboratory, NASA study finds Atlantic 'conveyor belt' not slowing, (2010). https://www.jpl.nasa.gov/news/nasa-study-finds-atlantic-conveyor-belt-not-slowing. Accessed 6 Feb 2024
7. Stommel, H.: An example of thermal convection. Transactions, American Geophysical Union **31**(4), 553–554 (1950). https://doi.org/10.1029/TR031i004p00553
8. Veronis, G.: Large-amplitude Bénard convection. J. Fluid Mech. **26**, 49–68 (1966). https://doi.org/10.1017/S0022112066001083
9. Vorovich, I.I., Youdovich, V.I.: Steady flow of a viscous incompressible fluid. Mat. Sb. **53**, 393–428 (1961)